

Ferromagnetic superconductivity driven by changing Fermi surface topology

K. G. Sandeman, G. G. Lonzarich¹ and A. J. Schofield²

¹*Low Temperature Physics Group, Cavendish Laboratory,
Madingley Road, Cambridge, CB3 0HE, United Kingdom.*

²*School of Physics and Astronomy, University of Birmingham,
Edgbaston, Birmingham B15 2TT, United Kingdom.*

We introduce a simple but powerful zero temperature Stoner model to explain the unusual phase diagram of the ferromagnetic superconductor, UGe_2 . Triplet superconductivity is driven in the ferromagnetic phase by tuning the majority spin Fermi level through one of two peaks in the paramagnetic density of states (DOS). Each peak is associated with a metamagnetic jump in magnetisation. The twin peak DOS may be derived from a tight-binding, quasi-one-dimensional bandstructure, inspired by previous bandstructure calculations.

I. INTRODUCTION

The predominance of spin singlet superconductors over their triplet counterparts has, in part, lead to the belief that superconductivity and magnetism are mutually exclusive—the upper critical field of a singlet superconductor is bounded by the Pauli paramagnetic limit. One might expect that a ferromagnet would be the natural stage for spin triplet superconductivity, where we could overcome Pauli limiting effects. But, until recently, there were no examples of ‘ferromagnetic superconductivity’ (FMSC)—the coexistence of itinerant ferromagnetism (FM) and superconductivity (SC) in a single bulk phase¹. This situation has changed with the observation of FMSC in UGe_2 ², URhGe ³ and ZrZn_2 ⁴. The behaviour of these materials is an example of a more general phenomenon; the observation of a novel state on the border of magnetism at low temperatures. By suppressing magnetic order by some control parameter, be it electron/hole density⁵ or external pressure⁶ physicists are now able to access regimes where magnetic fluctuations become quantum critical.

We choose here to concentrate on the case of UGe_2 , because whilst SC is only measurable in the ferromagnetic state (in common with URhGe and ZrZn_2), UGe_2 seems to possess particularly low electronic dimensionality, uniaxial magnetisation, and revealing features in the temperature-pressure phase diagram which we now review.

In Fig. 1 we show the temperature-pressure phase diagram for UGe_2 , with the Curie temperature T_C (suppressed to zero at pressure p_c) and superconducting transition temperature T_{SC} indicated^{2,7,8}. Another feature, T_x is also shown. This T_x shows up in measurements of lattice expansion¹⁰, as a jump in the low temperature T^2 component of the resistivity², as a small enhancement in specific heat⁸, as a kink in resistivity⁸ and as a change in the character of the Fermi surface as measured in de Haas van Alphen experiments¹¹. Most importantly for this work, T_x also appears as a slight jump in magnetisation⁸ which is sharpened at lower temperatures such that the low temperature moment has a step at pressure p_x in addition to the step at the quantum phase transition

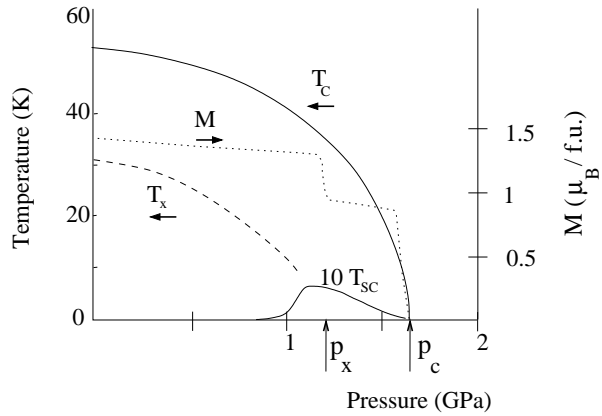


FIG. 1: The temperature-pressure phase diagram^{2,7,8} and low temperature easy axis magnetic moment, M (after Pfleiderer and Huxley⁹) of UGe_2 . T_{SC} is the superconducting transition temperature, scaled by a factor of 10 for clarity. T_C denotes the Curie temperature. T_x is a feature in the ferromagnetic state seen in various measurements, described in the text. M shows two transitions; one at p_x , corresponding to where the T_x line meets the pressure axis, and the other at the critical Curie pressure, p_c .

pressure, p_c (see Fig. 1). Furthermore, we note the close proximity of the $T_x(p)$ line to the peak in T_{SC} .

Most theories which describe ferromagnets close to a quantum phase transition have predicted that the superconducting transition temperature, T_{SC} should be at least as high in the paramagnetic state as it is in the ferromagnetic state. These theories have considered a electronically three-dimensional ferromagnet, either magnetically isotropic¹² or uniaxial¹³. Where theoretical models have predicted an enhancement of T_{SC} in the ferromagnetic regime, their basis seems unjustified in the case of UGe_2 . Kirkpatrick and coworkers¹⁴ have predicted an enhancement of the superconducting T_{SC} due to the coupling of magnons to the longitudinal magnetic susceptibility. However, the ferromagnetic state of UGe_2 is so magnetically anisotropic that the presence of transverse magnons seems an unlikely primary explanation for the enhancement of T_{SC} —at 4.2K and an external magnetic field of 4T, the magnetisation along the easy axis

is about 20 to 30 times that along either of the other crystallographic axes¹⁵. Other authors have drawn their inspiration from bandstructure calculations. Bandstructure analyses^{16,17,18} of UGe₂ seem to indicate that lowering temperature sparks the evolution of a quasi-two-dimensional majority carrier Fermi surface sheet below T_C . Furthermore there is the possibility that large sections of the quasi-two-dimensional Fermi surface may be parallel, making it almost one-dimensional. Until now, this low-dimensional magnetism has pushed authors in the direction of postulating the existence of a charge- or spin-density-wave state (CDW or SDW) below T_x ^{2,7}, sometimes by analogy with the α phase of uranium. Watanabe and Miyake¹⁹ have postulated that the interplay of CD or SD fluctuations at high wavevector will couple to the magnetisation, M in such a way as to enhance it at some critical value, M_x ³⁴. However, spin density fluctuations have yet to be observed in neutron experiments on UGe₂.

We turn to the low dimensional bandstructure for a different effect. The key idea will be that in a ferromagnet, somewhat uniquely, the magnetisation acts as a tuning parameter which can subtly change the topology of the *anisotropic* Fermi surfaces of different spin species. By contrast, in a rigid band picture of a paramagnetic metal, the Fermi surface is fixed. The added topological possibilities for a ferromagnet should be viewed as a useful tool—and as a reason for observing the enhancement of features, such as T_{SC} , within the ferromagnetic phase. This paper is planned as follows: firstly, we show that an electronic density of states (DOS) which has two peaks can reproduce the two steps in the observed low temperature magnetisation. We then show that the necessary form of DOS arises naturally from a low (quasi-one-) dimensional bandstructure and that the magnetisation resulting from this bandstructure has a jump in the ferromagnetic state which is coincident with the maximum in a superconducting instability, mediated by spin fluctuations.

II. MODEL

The simplest Stoner theory of magnetism is long-known to be inadequate in describing the temperature dependence of the magnetisation even of magnetically isotropic, electronically 3-dimensional ferromagnets, where spin fluctuations have to be taken into account. There, a fluctuation-averaged equation of state method, in the spirit of Lonzarich and Taillefer²⁰ or Yamada²¹ would be a improved model of magnetism at finite temperature, where we expect the temperature dependence of M to arise from the fluctuation response, rather than just the Fermi functions included in Stoner theory. The pronounced magnetic anisotropy of UGe₂ might ordinarily simplify matters, as the consequent absence of transverse spin modes will make a Stoner approach more valid, especially at low temperatures. How-

ever the reduced electronic dimensionality of UGe₂ will probably heighten the importance of spin fluctuations at finite temperatures.

We therefore circumvent finite temperature concerns by employing a *zero* temperature Stoner theory, with the first aim being to reproduce the step in $M(p)$ at p_x . We consider the action of pressure to be akin to that of varying the exchange energy, I in a Stoner model of the one-electron energy of separated majority (say, \uparrow) and minority (say, \downarrow) spin sheets: $E_{k\sigma} = \epsilon_k \pm IM$ ($-\uparrow, +\downarrow$). In this description, the occupation of each spin sheet σ is $n_\sigma = \int_{\epsilon_b}^{\mu_\sigma} \rho(\epsilon) d\epsilon$, where $M = \frac{1}{2}(n_\uparrow - n_\downarrow)$. Here ϵ_b is the bottom of the band, and spin σ occupies energy states up to μ_σ . The DOS is given by $\rho(\epsilon)$. We consider the total number of spins, $n_\uparrow + n_\downarrow = N$ to be fixed. The chemical potential, μ_σ of each spin sheet is therefore completely determined by the particular magnetisation and chosen electron number. The total energy density of the electron system is

$$F[M] = \int_{\epsilon_b}^{\mu_\uparrow} \rho(\epsilon) d\epsilon + \int_{\epsilon_b}^{\mu_\downarrow} \rho(\epsilon) d\epsilon + I\left(\frac{N^2}{4} - M^2\right) - g\mu_B H M, \quad (1)$$

where we have included a term for the presence of an external magnetic field, H .

Most phenomenological expansions of this energy density have included terms even in M , up to order M^6 . This can give one first order transition in $M(I)$. However, we are looking for an additional transition, corresponding to p_x , and believed to be first order⁹, although there is some controversy over this²². To have the possibility of an additional *first* order transition, we need the next even term in the Landau free energy expansion, thus obtaining an M^8 theory²³. We now show that a DOS with two peaks generically brings about the M^8 term in $F[M]$ by allowing a scenario where the global magnetisation can change rapidly, twice. We begin by taking a one-band DOS comprised of two Lorenztians, normalised such that the maximum number of electrons of each spin in the band is 1:

$$\rho(\epsilon) = \frac{\rho_0(\epsilon)}{\int_{\epsilon_B}^{\epsilon_T} \rho_0(\epsilon) d\epsilon} \quad (2)$$

where

$$\rho_0(\epsilon) = 1 + \frac{1}{a(\epsilon - b)^2 + 1} + \frac{1}{a(\epsilon + b)^2 + 1}, \quad (3)$$

where we can vary a to adjust the sharpness of the two humps and b to adjust their position. The humps are symmetric with respect to the zero energy and are centred on $\pm b$. We minimise $F[M]$, given by Eq. 1 with respect to magnetisation, M to obtain the variation of M with respect to the Stoner exchange, I . In Figure 2 we show plots of $M(I)$ for three sets of parameters a and b ,

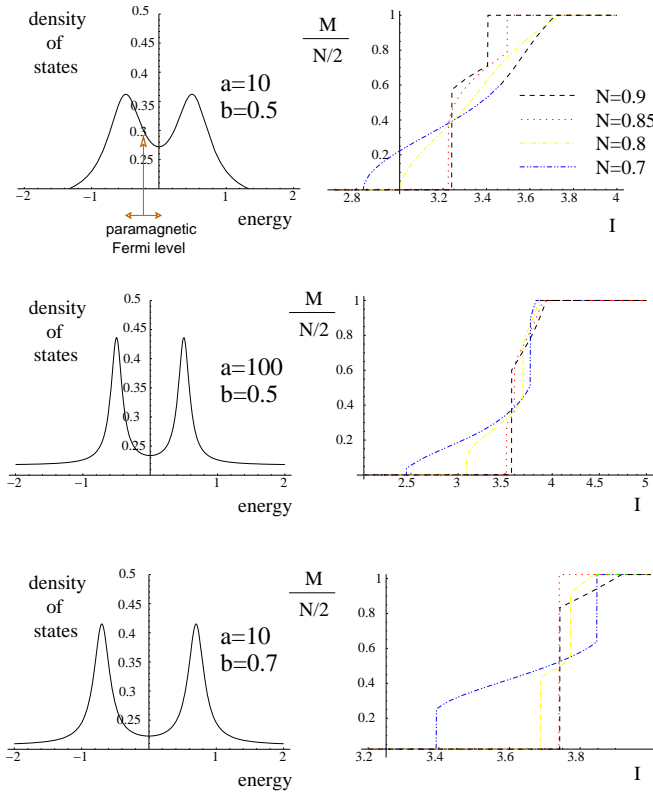


FIG. 2: Using the twin-peak density of states given by Eqs. 2 and 3, it is possible to obtain two transitions in the magnetisation of a Stoner ferromagnet, where the exchange parameter I is the varied quantity. We plot both the normalised density of states and the resultant $M(I)$ curve. If the two peaks in the DOS are too far apart, a saturated magnetic state is favoured. If the two peaks are too smooth, the transitions in $M(I)$ are weakened. The bandstructure parameters used in each case are indicated, together with the range of number of spins, N , used in the calculations of $M(I)$.

in each case setting the bottom and top, ϵ_B and ϵ_T of the band to be -2 and $+2$ respectively. For each set of parameters, we show the effect of varying the paramagnetic Fermi level, that is to say, the number of spins, N in the system, in the neighbourhood of half-filling. This places the paramagnetic Fermi level, μ_{EF} between the two DOS peaks. On increasing the exchange term, I , the spin sea is polarised and the majority Fermi level moves up from that of the paramagnetic state and the minority level moves down. The onset of ferromagnetism is governed by the usual Stoner criterion, $I\rho(\mu_{EF}) = 1$ in the case of a second order onset, or by the finite-magnetisation Stoner criterion²⁴ for a first order onset:

$$\frac{2IM}{\mu_{\uparrow} - \mu_{\downarrow}} = 1. \quad (4)$$

The finite magnetisation criterion holds for all M once the system is polarised, irrespective of the order of the onset. Each Fermi level feels the effect of the density of states peaks at different I , as long as the paramagnetic

Fermi level is off-centre with respect to the two DOS peaks. The main result is that, by making the density of states peaks sufficiently sharp and close together, *we can obtain two magnetic transitions, one from the paramagnetic state and another within the ferromagnetic state*. If the DOS peaks are too far apart, a saturated magnetic state is favoured; if the peaks are too smooth, the transitions in $M(I)$ are weakened and if the starting paramagnetic level is too close to the half-way point between the two peaks (N too close to 1) then only one transition is observed. Therefore, to observe two transitions, the paramagnetic filling level should be between the DOS peaks, but off-centre with respect to them.

A. Bandstructure phenomenology

Having shown that a double-humped DOS is perhaps key to understanding the magnetic properties of UGe_2 at low temperatures, we now set about working towards a tight-binding picture of the bandstructure of this compound which can reproduce both its magnetic and superconducting properties. There have been two major efforts towards bandstructure calculations of UGe_2 . The first, originally on a crystal structure with an incorrect space group was performed by Yamagami et al.¹⁷ and has since been revised¹⁸. This produced spin-separated Fermi sheets in the ferromagnetic state, centred on the Γ point, with the majority sheet strongly nested. The second approach, already mentioned, has been an LDA + U method, by Shick and Pickett¹⁶, using U as a fitting parameter for the zero temperature, ambient pressure magnetisation. Again, strongly nested Fermi sheets were obtained, but they were of mixed spin type and the sheet considered by those authors as being most important for superconductivity is centred on the crystallographic M point in their model. Furthermore, there was initial disagreement on the direction of the nesting vector \mathbf{Q} relative to the easy axis of magnetisation \mathbf{a} — both are ‘in-plane’, but Yamagami considered $\mathbf{Q} \perp \mathbf{a}$ whilst Shick found $\mathbf{Q} \parallel \mathbf{a}$. In summary, we take the following minimal, but key ingredients in our model:

- quasi-one-dimensional bandstructure (crucial to what follows)
- strong uniaxial magnetic anisotropy and
- spin-split Fermi sheets (even in the LDA + U work¹⁶, there is a large exchange splitting, of the order of 1 eV).

In our model, we utilise the interaction potential for spin fluctuation mediated pairing in the ferromagnetic state, as derived by Fay and Appel¹². We also follow their sign convention, namely that an attractive potential between like spins is positive. The interaction potential is heavily dependent on the Lindhard response, $\chi_{\sigma\sigma}^{(0)}(\mathbf{q})$

for the bandstructure under consideration:

$$V_{\sigma\sigma}(\mathbf{q}) = \frac{I^2 \chi_{-\sigma-\sigma}^{(0)}(\mathbf{q})}{1 - I^2 \chi_{\sigma\sigma}^{(0)}(\mathbf{q}) \chi_{-\sigma-\sigma}^{(0)}(\mathbf{q})}, \quad (5)$$

where I is again the repulsive Hubbard-type contact interaction acting between opposite spins and $\chi_{\sigma\sigma}^{(0)}(\mathbf{q})$ is given by

$$\chi_{\sigma\sigma}^{(0)}(\mathbf{q}) = \sum_{\mathbf{k}} \frac{f_{\sigma}^{(0)}(\mathbf{k}) - f_{\sigma}^{(0)}(\mathbf{k} + \mathbf{q})}{\epsilon(\mathbf{k} + \mathbf{q}) - \epsilon(\mathbf{k})}; \quad (6)$$

$f_{\sigma}^{(0)}(\mathbf{k})$ being the Fermi occupation function for spin σ which is at chemical potential μ_{σ} (μ_{σ} is defined previously). According to our chosen interaction mechanism, Eq. 5, a large $\chi_{\sigma\sigma}^{(0)}(\mathbf{q})$ might naively be expected to lead to an enhanced T_{SC} . However, the subtlety here is that the interaction potential in the ferromagnetic state mixes longitudinal susceptibilities of majority and minority spin sheets so the effect is not so clear-cut. We recall that in the free electron model, only in electronic dimensions less than two, there can be a peak in $\chi_{\sigma\sigma}^{(0)}(\mathbf{q})$ at non-zero \mathbf{q} ²⁵. In that case, we might expect that when one sheet of the Fermi surface is at optimal nesting, then perhaps $V_{\sigma\sigma}(\mathbf{q})$ will be highest. The problem with this argument is that a $V_{\sigma\sigma}(\mathbf{q})$ dominated by high- \mathbf{Q} modes would normally lead to very weak triplet pairing and in tight-binding approaches, finite \mathbf{q} peaks in $\chi_{\sigma\sigma}^{(0)}(\mathbf{q})$ are possible in two and three dimensions.

The approach we take is to look for density of states-driven superconductivity, where the large density of states giving rise to the magnetisation step at M_x is also able to enhance superconductivity in the ferromagnetic state. In tight-binding theory in two dimensions and lower, the peak in the density of states comes from the presence of a van Hove singularity. The simplest, familiar tight-binding bandstructure for the cuprates is of the form

$$\epsilon(\mathbf{k}) = -\alpha_x \cos k_x - \beta \cos k_x \cos k_y - \alpha_y \cos k_y \quad (7)$$

with $\alpha_x = \alpha_y = 1$ and β less than 1. This corresponds to equal nearest neighbour hopping in each of the two dimensions, and includes the next-nearest neighbour term, $\cos k_x \cos k_y$. This structure, as shown in Figure 3(a), has one van Hove singularity and is therefore of little use in studying the magnetic properties of UGe₂—as we have already found, we require *two* density of states peaks. However, as we will now show, if we now reduce the amplitude of the $\cos k_y$ term, we cross over into quasi-one-dimensions and begin to lift the degeneracy of the van Hove contours, giving two of the them, with adjustable separation.

The most common quasi-1D bandstructure in the literature is probably

$$\epsilon(\mathbf{k}) = -\alpha_x \cos k_x - \alpha_y \cos k_y \quad (8)$$

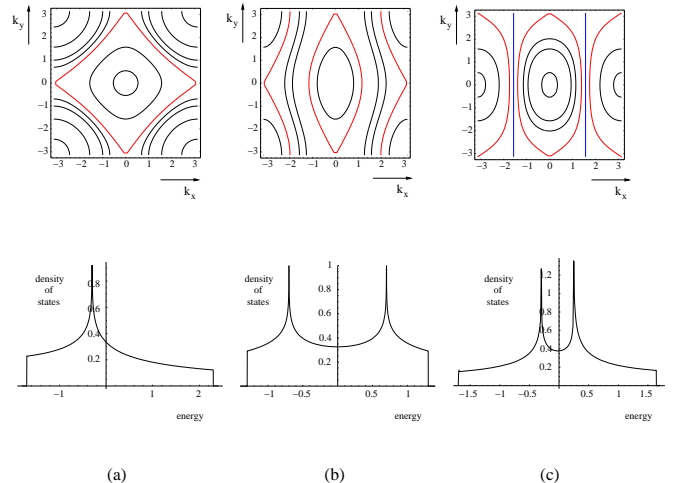


FIG. 3: Two dimensional and quasi-one-dimensional tight-binding bandstructures: contour plots (top row of figures) with the van Hove contours shown in red and associated densities of states (bottom row). In (a) the two-dimensional structure given by Eq. 7 with $\alpha_x = \alpha_y = 1$ and $\beta = -0.3$ is shown. This is a structure most often studied in connection with the cuprates. In (b) we show the quasi-one-dimensional structure of Eq. 8 with $\alpha_x = 1, \alpha_y = 0.3$. In (c), higher harmonics in the principal direction are included (Eq. 9) with $\alpha_x = 1, \beta = 0.7, \delta = 0.03$ and $\gamma = -0.03$. We see that in (a) there is one (degenerate) van Hove contour, but on going into quasi-one-dimensions, we lift this degeneracy and find two van Hove contours and hence two maxima in the density of states. Furthermore, the choice of bandstructure in (c) has an optimal nesting scenario (shown in blue) which is separate from both of the van Hove contours, due to the elimination of the $\cos k_y$ term in the bandstructure.

which is used to describe some organic superconductors. Here, α_x is 1 and α_y is less than 1 and the model corresponds to nearest neighbour hopping in each of the two dimensions. This bandstructure has two van Hove contours (see Figure 3(b)) and hence two density of states peaks. Thus, on tuning our magnetisation, we can observe in both spin types the transition through a van Hove singularity in the density of states at the Fermi level, provided, as stated before, that our paramagnetic Fermi level is between the two peaks in the density of states. The problem arises that when the peaks are close enough together to cause an effect in the magnetisation curves, the variation of the DOS in between them is not very rapid. This leads to a weakening of the transitions in $M(I)$ as found with a slowly varying Lorentzian DOS in the last section.

However, if we assume a quasi-one-dimensional dispersion of the form

$$\epsilon(\mathbf{k}) = -\alpha_x \cos k_x - \beta \cos k_x \cos k_y - \gamma \cos 2k_x - \delta \cos 3k_x \quad (9)$$

with $\alpha_x = 1$ and β, γ, δ all less than unit magnitude, we will be able to explore the possibility of two, first order jumps in $M(I)$.

The higher harmonics in the principal direction k_x and the next-nearest term, $\cos k_x \cos k_y$ which appear in Eq. 9 are not unreasonable in a system which we know to be strongly one-dimensional in character. The nearest neighbour term in k_y has been reduced to zero. As shown in Figure 3(c), this dispersion relation yields two van Hove contours (and hence maxima in electronic density of states), and also goes through a perfect nesting scenario.³⁵ We note that our choice of bandstructure is based on an extrapolation from the one point ($T = 0$, $p = 0$) of the phase diagram calculated in Refs.^{16,17,18}, with the idea being that there should be strong nesting present at full magnetisation in our model, to match the bandstructure calculations. Indeed, the high energy contours of this dispersion are fairly well nested (Figure 3(c)). To achieve a magnetically saturated state which does not completely fill the band, we require less than half-filling of the band in the paramagnetic state, a requirement which is in line with the demands of the $M(I)$ profile from Section II. Our choice of bandstructure will ultimately help to link p_x , the maximum in T_{SC} and the mass enhancement observed in de Haas van Alphen measurements. First we concentrate on the magnetisation as a function of Stoner exchange, I .

III. RESULTS

A. Two jumps in magnetisation from a tight-binding bandstructure

Taking the quasi-one-dimensional bandstructure given by Eq. 9 and varying parameters β , γ , and δ , we obtain the variation of zero temperature magnetisation with exchange interaction I as we did for Lorentzian densities of states.³⁶ In Figure 4, we present $M(I)$ for different total numbers of electrons, N below half-filling in the case of four different sets of tight-binding parameters. In each case, the paramagnetic Fermi level sits in between the two peaks in the DOS. Initial polarisation at I_c (labelled by analogy with p_c in experiment) is first order—this is due to the minority sheet approaching the lower van Hove peak as polarisation commences.

There are several features to be noted from the plots in Fig. 4. Firstly, as in Fig. 2, if N is below half-filling, a second magnetic transition can occur when the majority spin sheet feels the effect of the upper peak in the DOS. However, when N is too close to half filling, or when the dip between the two density of states peaks is too sharp, we get only one first order transition, which can even be straight to saturation magnetisation. Once again, in order to observe the *two* transitions seen in UGe₂, one should have a paramagnetic Fermi level which is off-centre with respect to two DOS peaks. Secondly, the upper transition (which we henceforth label I_x by analogy with p_x from experiment), can either be to finite magnetisation (and either first order or beyond the first order critical point) or can be first order

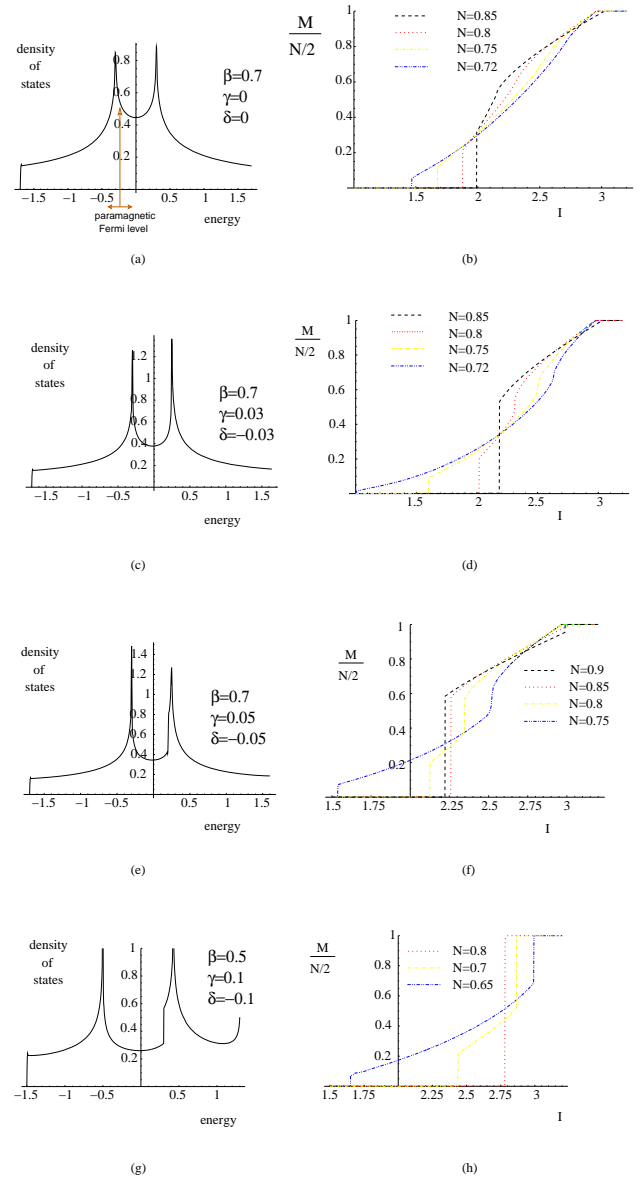


FIG. 4: A set of phenomenological quasi-one-dimensional dispersions for UGe₂, where both the possibility of tuning the magnetisation through a van Hove singularity and a perfect nesting condition are present. (a), (c), (e) and (g) show the calculated density of states whilst (b), (d), (f) and (h) are the calculated graphs of magnetisation as a function of I , the Stoner exchange parameter for various levels of band-filling, below half-filling. The tight-binding parameters for our dispersion, $\epsilon(\mathbf{k}) = -\cos k_x(1 + \beta \cos k_y) - \gamma \cos 2k_x - \delta \cos 3k_x$ are indicated. As in Fig. 2, two magnetic transitions are often visible.

to saturation magnetisation. According to Eq. 5, a transition to saturation magnetisation would naturally kill any magnetically-mediated superconductivity due to the lack of one spin species. Thus we turn our attention to an upper transition not of saturating nature, and which could be first order, or close to first order, as the latter would allow the Fermi surface sheet configurations to be

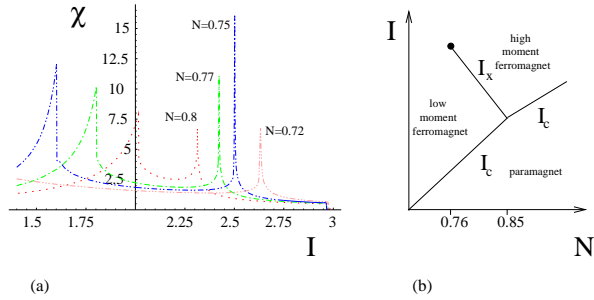


FIG. 5: The phase diagram of our model in N, I space shows a line of first order transitions at $I_x(N)$ which end in a critical point. The transitions at the Curie onset, I_c are also first order. This can be seen in the behaviour of (a) the longitudinal susceptibility and (b) the resulting (approximate) phase diagram. The tight-binding parameters used here are $\beta = 0.7$, $\gamma = 0.03$ and $\delta = -0.03$, in line with what follows.

explored as the magnetisation is tuned by temperature or pressure, allowing the presence of sharp peaks in the density of states to be observed in measurements such as heat capacity and resistivity.

The above considerations make the second example in Fig. 4 a most useful candidate, as we have the option of the upper transition being first order or close to first order, depending on N , and the magnetisation does not saturate at the upper transition. Henceforth, we take $\beta = 0.7$, $\gamma = 0.03$ and $\delta = -0.03$.

Interestingly, the magnetic phase diagram in the N, I plane seems to contain a line of first order transitions corresponding to $I_x(N)$. This line terminates at a critical point at a value of N of about 0.76. For values of N below this, the transition in $M(I)$ is smooth and can be described as close to first order. This is perhaps best seen in Figure 5(a), where we show the longitudinal susceptibility, χ as a function of I for $\beta = 0.7$, $\gamma = 0.03$ and $\delta = -0.03$, taking different values of N . We take the longitudinal susceptibility from the Stoner forms:

$$\chi_{para} = \frac{\rho(\mu_{EF})}{1 - I\rho(\mu_{EF})}, \quad (10)$$

$$\chi_{ferro} = \frac{2\rho(\mu_{\uparrow})\rho(\mu_{\downarrow})}{\rho(\mu_{\uparrow}) + \rho(\mu_{\downarrow}) - 2I\rho(\mu_{\uparrow})\rho(\mu_{\downarrow})} \quad (11)$$

in the paramagnetic (Fermi level μ_{EF}) and ferromagnetic states, respectively. As seen in Figure 5(a), the susceptibility at I_x grows as we move closer to the critical point; the resulting (approximate) phase diagram in (N, I) space is shown in Figure 5(b).

B. Magnetic field effects

It has also been found that the features associated with T_x and T_c can be recovered at pressures above p_x and p_c respectively by the application of a magnetic field. In

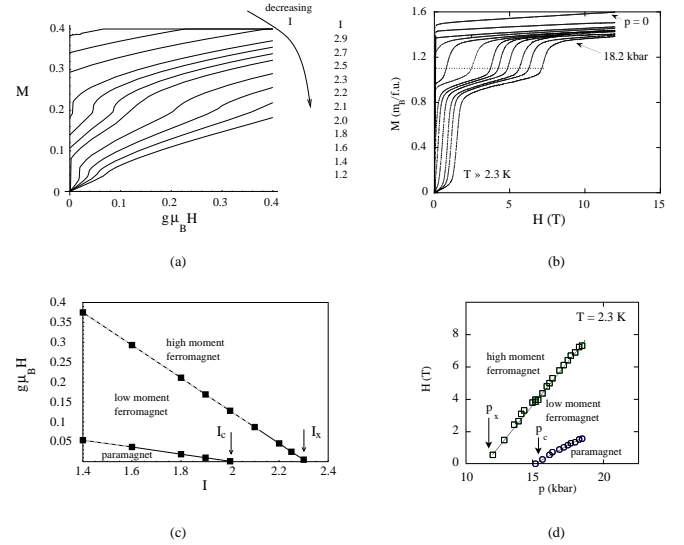


FIG. 6: Our model predicts that both the magnetic jump at the onset of ferromagnetism and that at finite magnetisation can be pushed to lower values of exchange energy I_c or I_x respectively (corresponding to pressures higher than p_c and p_x) by the application of a magnetic field, H . The tight-binding parameters used here are again $\beta = 0.7$, $\gamma = 0.03$ and $\delta = -0.03$. The number of spins, N is 0.8 in both figures (a) and (c) which show the calculated $M(I)$ curves and the resulting phase diagram in H, I space. Recent experimental data, from Pfleiderer and Huxley⁹ is shown in (b) and (d). This has a form similar to that predicted in (a) and (c), with the appearance of two transitions in M , which are tunable with pressure.

our model, this metamagnetism arises as a direct consequence of having spin-split Fermi surfaces, with the spin species being governed by number conservation and the free energy of the form given in Eq. 1. As shown in Fig. 6, turning on the magnetic field, H , pushes both the magnetisation jump at I_c (the Curie transition) and at I_x (within the ferromagnetic state) to lower values of I , or equivalently, higher pressures. Both the predicted $M(I)$ curves and the resulting phase diagram in H, I space bear a striking resemblance to recent experimental data⁹. We should point out that the calculated H, I phase diagram was obtained by looking for the maximum in the gradient of the magnetisation for each $M(I)$ plot in field. The first order nature of both transitions is softened with decreasing I —corresponding to going to higher pressures. Experimentally, such softening is not observed at pressures reached this far, as can be seen from Figure 6(b). We indicate where the magnetic transition in our model is no longer first order by a dotted line on the H, I phase diagram.

C. Superconductivity and the zero-temperature phase diagram

From the heavy nature of the quasiparticles alone, we expect strong coupling theory to be required to gain a true estimate of T_{SC} in UGe₂. However, we can gain useful information on the form of the phase diagram from examining the zero temperature, weak-coupling properties of our model. We note here that, without a reliable model of $M(T)$, it is impossible to construct the usual T_{SC} equation in the BCS theory in the ferromagnetic state, as here we have an example of a temperature-dependent potential—the changing magnetisation alters the spin-dependent interaction.

A reasonable estimate of the strength of triplet pairing can be gained from examining the relative magnitudes of the mass renormalisation parameter λ_Z and interaction parameter λ_Δ , defined as

$$\lambda_Z = \frac{\int_{FS} \int_{FS'} d^2k d^2k' V_{\uparrow\uparrow}(\mathbf{k} - \mathbf{k}')}{\int_{FS} d^2k}, \quad (12)$$

$$\lambda_\Delta = \frac{\int_{FS} \int_{FS'} d^2k d^2k' V_{\uparrow\uparrow}(\mathbf{k} - \mathbf{k}') \eta(\mathbf{k}) \eta(\mathbf{k}')}{\int_{FS} d^2k \eta^2(\mathbf{k})}, \quad (13)$$

where each integration is over the Fermi surface (FS) either in \mathbf{k} or \mathbf{k}' space. The term $\eta(\mathbf{k})$ is the angular part of the superconducting order parameter. In the above we are following the notation adopted by Monthoux and Lonzarich²⁶ and *restrict ourselves to examine majority spin triplet pairing*, using $V_{\uparrow\uparrow}(\mathbf{q})$. The choice of order parameter should naturally reflect the symmetry properties of the UGe₂ crystal structure. Such considerations should lead us to examine non-unitary states^{27,28}, but here for simplicity we consider as an example the states $\Delta_{\mathbf{k}} = \Delta_0 \sin(k_x)$ and $\Delta_0 \sin(k_y)$, anticipating that which state is favoured may change as the majority Fermi surface is tuned through p_x , making the transition from being open to being closed. The favoured state is determined by which $\eta(\mathbf{k})$ gives a larger positive value of λ_Δ .

There is a caviat at this stage. The sharpness of the van Hove singularities is useful in providing the magnetisation behaviour shown in Section III A. However, as can be readily seen from Eq. 5, it can also lead to a switching of the sign of the pair interaction from attraction to repulsion at zero \mathbf{q} if the density of states at the van Hove point is *too* high. This is because $\chi_{\sigma\sigma}^{(0)}(\mathbf{q} = 0) = \rho(\mu_\sigma)$. With the presence of a strict low dimensional van Hove singularity (an infinity in the DOS) at zero temperature, the quantity $\rho(\mu_\uparrow)\rho(\mu_\downarrow)$ will be greater than 1 when the majority Fermi level reaches the van Hove point.

There are several possible routes to softening the van Hove singularity. One would be to introduce a small amount of disorder into the model. Another would be to transfer the calculation to three electronic dimensions, rather than the current two, but that is computationally time-consuming. Here we take a simpler

approach, calculating all $\chi_{\sigma\sigma}^{(0)}(\mathbf{q})$ at a small finite temperature ($k_B T = 0.045$), retaining the original zero-temperature value of I for each magnetisation examined. This procedure maintains the order of the magnetic transition at I_x , although it does mean that the effective density of states, $\chi_{\sigma\sigma}^{(0)}(\mathbf{q} = 0)$ is inconsistent with that used to find $M(I)$. $\chi_{\sigma\sigma}^{(0)}(\mathbf{q})$ is calculated on a 40 by 40 grid for \mathbf{k} and \mathbf{k}' points in the Brillouin zone. The agreement is close away from the van Hove regions.

In order to have two first order magnetic phase transitions (see Fig. 5(b)), we take $N = 0.77$ in what follows, and examine majority sheet, spin triplet superconductivity. The final refinement to the model comes in the form of adjusting the \mathbf{q} -dependence of I at this stage. Until now, we have considered a \mathbf{q} -independent Stoner factor which arises from on-site repulsion of like-spin electrons. However, I should really convey some of the physics of electron-electron interactions at finite distances, and so, in calculations of the superconducting potential, we convert to the following form:

$$I \rightarrow \frac{I}{1 + \xi q^2} \quad (14)$$

which effectively reduces high- \mathbf{q} modes in the system, in line with the ferromagnetism of the real compound. This is the simplest, first approximation of such effects.

In Fig. 7 we show a measure of the superconducting interaction strength, $\frac{\lambda_\Delta}{1 + \lambda_Z}$, for various values of ξ , our Stoner ‘structure factor’. The term $1 + \lambda_Z$ measures the mass renormalisation—this is shown separately in Fig. 8. Of course, $\frac{\lambda_\Delta}{1 + \lambda_Z}$ is not the full story when one considers how the superconducting transition temperature T_{SC} should behave as a function of I . Roughly speaking, $T_{SC} \sim \omega_c e^{-(\frac{1 + \lambda_Z}{\lambda_\Delta})}$ (see, for example, Fay and Appel¹²) and there is substantial variation of ω_c , the paramagnon energy with I , especially when soft magnetic modes are present. The paramagnon energy can be expanded as

$$\omega_c \sim \zeta q (\chi^{-1} + cq^2), \quad (15)$$

where ζ and c are temperature dependent parameters, equivalent to γ and c in the work of Lonzarich²⁹. As developed by Brinkman and Engelsberg³⁰ and implemented by Fay and Appel, the ω_c prefactor will substantially reduce superconductivity at the ferromagnetic I_c and the same argument should apply around the secondary transition at I_x , although in both cases this effect is more drastic for a second order magnetic transition (where the susceptibility diverges, i.e. $\chi^{-1} \rightarrow 0$) than for the first order cases here. What remains important, therefore, is the *stable region of superconductivity in the ferromagnetic state*, where $\frac{\lambda_\Delta}{1 + \lambda_Z}$ is approximately flat and high, especially for higher Stoner structure factor, ξ .

We might reasonably ask what it is that enhances superconductivity in the region between I_x and I_c . In this range of I , the majority Fermi level sits between the two van Hove peaks, and an examination of the \mathbf{q} dependence of the interaction potential, Eq. 5 reveals that there is a

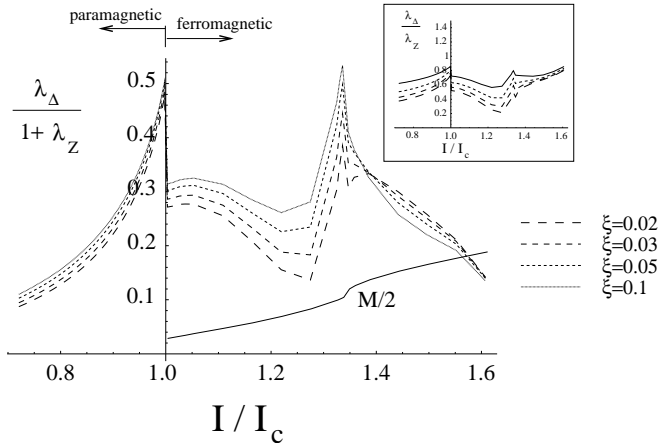


FIG. 7: A measure of the strength of superconductivity: $\frac{\lambda_\Delta}{1+\lambda_Z}$ as a function of Stoner interaction strength, I , normalised with respect to I_c , the value of I at the zero temperature Curie point. I_x , the value of I for the second jump in magnetisation, akin to the pressure identified as p_x in UGe₂, gives rise to the peak at $I_x/I_c \sim 1.34$. Also shown is the magnetisation, scaled down by a factor of two in the dimensionless units we are using. The inset shows the ratio $\frac{\lambda_\Delta}{\lambda_Z}$ is always less than 1, as expected. In both plots, we show the results for different values of ‘Stoner structure factor’, ξ (Eq. 14). The tight-binding parameters used here are again $\beta = 0.7$, $\gamma = 0.03$ and $\delta = -0.03$, and the number of spins, $N = 0.77$.

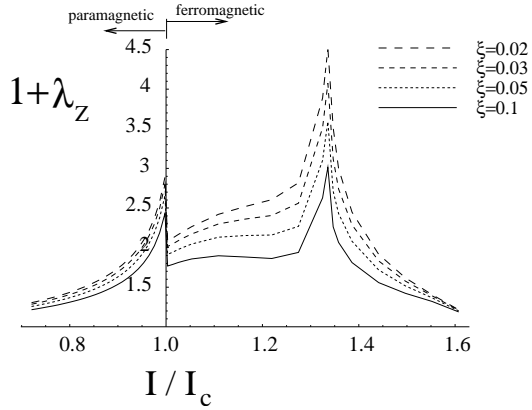


FIG. 8: The mass renormalisation: $1 + \lambda_Z$ as a function of Stoner interaction strength, I , normalised with respect to I_c , the value of I at the zero temperature Curie point. This quantity peaks in the ferromagnetic state and remains high with decreasing I into the paramagnetic state. Again, we show the results for different values of ‘Stoner structure factor’, ξ . The tight-binding parameters used here are again $\beta = 0.7$, $\gamma = 0.03$ and $\delta = -0.03$. The number of spins, $N = 0.77$.

region of high, sustained zero \mathbf{q} pairing for $I_c < I < I_x$.³¹ At both I_c and I_x , $V(\mathbf{q})$ is broad and high around $\mathbf{q} = 0$. Outwith the region $I_c < I < I_x$ the pairing potential is smaller and more localised around zero \mathbf{q} . Furthermore, in the region between I_c and I_x , the mass renormalisation, represented by λ_Z is also approximately flat and high. This mass enhancement, shown in Fig. 8 com-

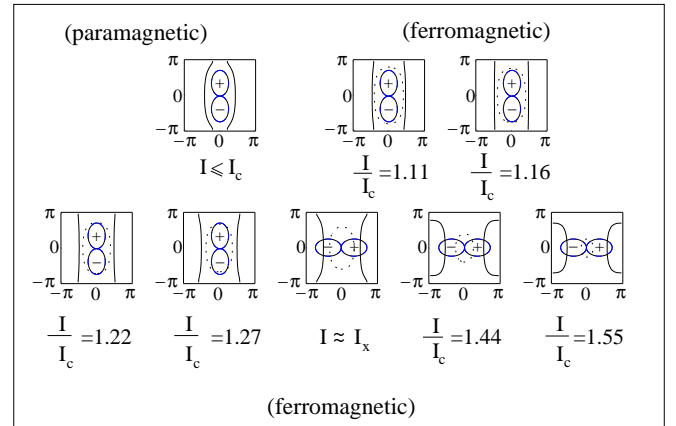


FIG. 9: Evolution of majority (solid line) and minority (dotted line) Fermi surfaces as a function of Stoner exchange. We see the transition in the majority sheet from an open to a closed morphology, going through a van Hove singularity at $I = I_x$. Also shown is the order parameter used, which changes from $\sin(k_y)$ for $I < I_x$ to $\sin(k_x)$ for $I > I_x$. The tight-binding parameters used here are again $\beta = 0.7$, $\gamma = 0.03$ and $\delta = -0.03$, and the number of spins, $N = 0.77$.

pares well with the high effective mass plateau found in de Haas van Alphen measurements on the ferromagnetic state between pressures p_c and p_x .

Lastly we note that the order parameter, $\eta(\mathbf{k})$ favoured on tuning I , changes as we go through I_x . This makes sense from the point of view of the Fermi surface topology, as depicted in Figure 9. $\eta(\mathbf{k}) = \sin(k_y)$ is favoured when the majority spin sheet is open—for all $I < I_x$ —and the $\sin(k_x)$ order parameter becomes favoured for the closed surfaces for $I > I_x$. As already stated, these are overly simplified gap functions, so this change of symmetry may well be more gradual or masked in a non-unitary representation.

IV. CONCLUSIONS

In this paper we have proposed that the unusual phase diagram of UGe₂ is a result of a novel tuning of the Fermi surface topology by the magnetisation of the ferromagnetic state. We have constructed a model for this which illustrates how superconductivity, the tunable magnetisation features and the quasiparticle mass are related by a twin-peak density of states feature, consistent with experiment.

We have first looked for an explanation of the two transitions in the low temperature magnetisation of UGe₂. We have shown how a density of states with two peaks as a function of energy will give rise generically to a zero temperature magnetisation which has two transitions as the ratio of Stoner exchange energy to bandwidth is tuned. We have demonstrated how this interesting form of DOS arises when the bandstructure is quasi-one-dimensional, as is believed to be the case for UGe₂.

We are thus able to propose a mechanism for the asymmetry of the superconducting T_{SC} with respect to the magnetic quantum phase transition associated with the Curie temperature, shifting the focus of our attention away from p_c towards p_x as the magnetic transition point of interest with regard to superconductivity. In our model, a large density of states at the majority spin Fermi surface is associated with the T_x transition and is also driving superconductivity. This causes superconductivity to be favoured in the ferromagnetic state relative to the paramagnetic state in a natural and previously overlooked way, and could also be a reason for the enhancement of superconductivity in the ferromagnetic state of other materials. We further note that, in a real system, the presence of impurities will probably enhance further the relative tendency to formation of the

superconducting state in the ferromagnetic phase.

There is also a straightforward explanation in the band magnetism scenario for the observed metamagnetic behaviour and a large, constant mass enhancement between I_x and I_c , consistent in form with de Haas van Alphen measurements. Potentially we may have a reason for the disappearance of dHvA signal between p_x and p_c , which would here be due to the Fermi surface becoming open. However, we should note that only one set of authors have observed such disappearance of dHvA signal³².

KGS wishes to thank C. Bergemann, J. Flouquet, A.D. Huxley, S.R. Julian, A.A. Katanin, D.E. Khmelnitskii, P.B. Littlewood, A.J. Millis, P. Monthoux, C. Pfleiderer, S.S. Saxena, T. Schmidt, M. Sigrist and T. Terashima for useful discussions. Financial support was supplied by the EPSRC.

¹ J. Flouquet and A. Buzdin, Physics World **15** (1):9 (2002).

² S. S. Saxena et al., Nature (London) **406**, 587 (2000).

³ D. Aoki et al., Nature (London) **413**, 613 (2001).

⁴ C. Pfleiderer et al., Nature (London) **412**, 58 (2001).

⁵ H.V. Löhneysen et al., J. Phys. Soc. Jpn. **69**, 63-70 (2000).

⁶ N. D. Mathur et al. Nature (London) **394**, 39 (1998).

⁷ A. D. Huxley et al., Phys. Rev. B **63**, 144519 (2001).

⁸ N. Tateiwa et al., J. Phys. C. **13**, L17-L23 (2001).

⁹ C. Pfleiderer and A. D. Huxley, Phys. Rev. Lett. **89**, 147005 (2002).

¹⁰ G. Oomi et al., Physica B **186-188**, 758 (1993).

¹¹ T. Terashima et al., Phys. Rev. Lett. **87**, 166401 (2001).

¹² D. Fay and J. Appel, Phys. Rev. B **22**, 3173 (1980).

¹³ R. Roussev and A. J. Millis, Phys. Rev. B **63**, 140504(R) (2001).

¹⁴ T. R. Kirkpatrick et al., Phys. Rev. Lett. **87**, 127003 (2001).

¹⁵ Y. Onuki et al., J. Phys. Soc. Jpn. **61**, 293 (1992).

¹⁶ A. B. Shick and W. E. Pickett, Phys. Rev. Lett. **86**, 300 (2001).

¹⁷ H. Yamagami and A. Hasegawa, Physica B **186-8**, 182 (1993).

¹⁸ S. Tejima, H. Yamagami and N. Hamada, *unpublished*.

¹⁹ S. Watanabe and K. Miyake, Physica B **312**, 115 (2002), J. Phys. Chem. Solids **63**, 1465 (2002), *private communication* and *unpublished*: cond-mat/0110492.

²⁰ G. G. Lonzarich and L. Taillefer, J. Phys. C **18**, 4339 (1985).

²¹ H. Yamada, Phys. Rev. B **47**, 11211 (1993).

²² T. Terashima et al., Phys. Rev. B **65**, 174501 (2002).

²³ M. Shimizu, J. Physique **43**, 155 (1982).

²⁴ P. Fazekas, *Lecture Notes on Electron Correlation and Magnetism* (World Scientific, Singapore, 1999), p. 408.

²⁵ G. Grüner, *Density Waves in Solids* (Addison Wesley, 1994).

²⁶ P. Monthoux and G. G. Lonzarich, Phys. Rev. B **63**, 054529 (2001).

²⁷ K. Machida and T. Ohmi, Phys. Rev. Lett. **86**, 850 (2001).

²⁸ I. A. Fomin, JETP Lett. **74**, 111 (2001).

²⁹ G. G. Lonzarich in *Electron* (ed. M. Springford), Chapter 6 (Cambridge University Press, Cambridge, 1997).

³⁰ W. F. Brinkman and S. Engelsberg, Phys. Rev. **169**, 417 (1968).

³¹ K. G. Sandeman, Ph.D. thesis, University of Cambridge, 2002.

³² R. Settai et al., J. Phys. C. **14**, L29 (2002).

³³ J. R. Schrieffer, X. G. Wen and S. C. Zhang, Phys. Rev. B **39**, 11663 (1989).

³⁴ By coupling high wavevector fluctuations to the $\mathbf{q} = 0$ mode, Watanabe and Miyake's model is reminiscent of the spin-bag mechanism of nodeless superconductivity proposed by Schrieffer et al. in the context of the cuprates³³.

³⁵ It is worth noting that, on scanning through energy in *quasi*-one-dimensions, optimal nesting (which is also the density of states minimum) does *not* coincide with the van Hove point (the density of states maximum). This is because optimal nesting in quasi-1D results from a Fermi surface consisting of parallel lines, each parallel to one axis of the Brillouin zone, as shown by the blue lines in Figure 3(c). By contrast, the optimal nesting Fermi surface of a two-dimensional square lattice in a nearest-neighbour tight-binding model is a diamond shape, with parallel surfaces at 45 degrees to the Brillouin zone axes. As shown in Figure 3(a), this Fermi surface also corresponds to the van Hove point and density of states maximum.

³⁶ Setting α_x to 1 in Eq. 9 and varying I is equivalent to varying the quantity $I' = I/\alpha_x$, as can be seen from the form of the free energy in Eq. 1. The effect of increasing pressure is to increase, probably most strongly, the hopping parameter α_x . This suppresses ferromagnetism, as it reduces I' . We show plots of $M(I)$ since $I = I'$ here.